Psychopharmacology (2012) 221:101–113
DOI 10.1007/s00213-011-2553-4

ORIGINAL INVESTIGATION

# Quinpirole elicits differential in vivo changes in the pre- and postsynaptic distributions of dopamine $D_2$ receptors in mouse striatum: relation to cannabinoid-1 ($CB_1$) receptor targeting

**Diane A. Lane · June Chan · Megan L. Fitzgerald · Chris S. Kearn · Ken Mackie · Virginia M. Pickel**

Received: 14 April 2011 / Accepted: 16 October 2011 / Published online: 8 December 2011


**Abstract**
*Rationale* The nucleus accumbens (Acb) shell and caudate-putamen nucleus (CPu) are respectively implicated in the motivational and motor effects of dopamine, which are mediated in part through dopamine $D_2$-like receptors ($D_2$Rs) and modulated by activation of the cannabinoid-1 receptor ($CB_1$R). The dopamine $D_{2/D3}$ receptor agonist, quinpirole elicits internalization of $D_2$Rs in isolated cells; however, dendritic and axonal targeting of $D_2$Rs may be highly influenced by circuit-dependent changes in vivo and potentially influenced by endogenous $CB_1$R activation.

*Objective* We sought to determine whether quinpirole alters the surface/cytoplasmic partitioning of $D_2$Rs in striatal neurons in vivo.
*Methods* To address this question, we examined the electron microscopic immunolabeling of $D_2$ and $CB_1$ receptors in the Acb shell and CPu of male mice at 1 h following a single subcutaneous injection of quinpirole (0.5 mg/kg) or saline, a time point when quinpirole reduced locomotor activity.
*Results* Many neuronal profiles throughout the striatum of both treatment groups expressed the $D_2$R and/or $CB_1$R. As compared with saline, quinpirole-injected mice showed a significant region-specific decrease in the plasmalemmal and increase in the cytoplasmic density of $D_2$R-immunogold particles in postsynaptic dendrites without $CB_1$R-immunolabeling in the Acb shell. However, quinpirole produced a significant increase in the plasmalemmal density of $D_2$R immunogold in $CB_1$R negative axons in both the Acb shell and CPu.
*Conclusions* Our results provide in vivo evidence for agonist-induced $D_2$R trafficking that is inversely related to $CB_1$R distribution in postsynaptic neurons of Acb shell and in presynaptic axons in this region and in the CPu.

**Keywords** Marijuana · Motor inhibition · Reward · Drug addiction · Nucleus accumbens shell · Caudate-putamen nucleus

Associate editor: A. Leslie Morrow, PhD; Molecular Psychopharmacology

Chris S. Kearn, deceased February 19, 2009

D. A. Lane · J. Chan · M. L. Fitzgerald · V. M. Pickel
Department of Neurology and Neuroscience,
Weill-Cornell Medical College,
New York, NY 10065, USA

C. S. Kearn
Department of Anesthesiology, University of Washington,
Seattle, WA 98195, USA

K. Mackie
Department of Psychological and Brain Sciences, MSBII 120,
Indiana University,
702 N Walnut Grove Ave,
Bloomington, IN 47405-2204, USA

V. M. Pickel (✉)
Department of Neurology and Neuroscience,
Cornell University Medical College,
407 East 61st St,
New York, NY 10065, USA
e-mail: vpickel@med.cornell.edu

## Introduction

Dopamine acts through $D_1$ and $D_2$-like receptors ($D_2$Rs) that are highly expressed in neurons located within both the

shell and core compartments of the nucleus accumbens (Acb) and in the dorsal striatum, caudate-putamen nucleus (CPu; Durstewitz et al. 2000; Missale et al. 1998; Noble 2003; Yao et al. 2008). Of these striatal receptors, the $D_2$Rs are particularly important because of their involvement in impulsivity (Besson et al. 2010; Lee et al. 2009) and in the beneficial and adverse motor side effects produced by classic antipsychotic drugs, all of which are $D_2$R blockers (Artigas 2010; Schlagenhauf et al. 2008; Soiza-Reilly and Azcurra 2009).

The motor effects mediated through $D_2$Rs may be ascribed not only to signaling in striatal neurons, but also to the presynaptic inhibition of the release of dopamine and other neurotransmitters from axon terminals derived from extrinsic neurons (Bamford et al. 2004; Delle Donne et al. 1997; Hersch et al. 1997; Wang et al. 2006). In the Acb shell, $D_2$Rs are present in mesolimbic dopaminergic and prefrontal cortical glutamatergic terminals consistent with their role in modulation of cortico-striatal transmission involved in motivated behaviors (Del Arco and Mora 2009; Sesack and Grace 2010). In contrast to the Acb shell, many of the $D_2$Rs in the dorsolateral CPu are located on somatosensory cortical and nigrostriatal dopaminergic axons, where their activation can profoundly affect the learning of motor habits (Kienast and Heinz 2006; Schlagenhauf et al. 2008). Thus, many of the diverse behavioral effect ascribed to quinpirole and other $D_2$R agonists are mediated through region-specific neural networks within the Acb shell and CPu. In each region, however, activation of the $D_2$R may largely modulate glutamatergic and dopaminergic transmission (Ikemoto 2002; Lee et al. 2009; Van Hartesveldt et al. 1992).

An intricate, yet potentially indirect, relationship exists between the dopamine and cannabinoid systems. Many neurons in the dorsal striatum and Acb co-express dopamine $D_2$ and cannabinoid $CB_1$ receptors, and systemic administration of the dopamine $D_{2/3}$R agonist LY171555 (quinpirole) occurs with a concurrent upregulation of endocannabinoid (anandamide) signaling (Giuffrida et al. 1999; Swanson et al. 1997; van der Stelt and Di 2003; Van Hartesveldt 1997). Increased $CB_1$R activation augments quinpirole-induced changes in locomotor activity (Gorriti et al. 2005) suggesting that activation of $D_2$Rs may be mediated by subsequent activation of the endocannabinoid system (Martin et al. 2008). Moreover, co-activation of these receptors, in vitro, produces changes in intracellular signaling cascades due to heterodimerization of these two receptor types (Kearn et al. 2005; Glass and Felder 1997). As such, dopaminergic activation may differ depending upon presence or absence of CB1 receptors. In vitro studies of cultured cells and isolated neurons show that agonist-activated $D_2$Rs are rapidly internalized and either degraded or recycled to the plasma membrane (Kim et al. 2008; Namkung et al. 2009; Skinbjerg et al. 2010) (Xiao et al. 2009). In vivo, however, the $D_2$R subcellular distribution may be influenced not only by agonist activation in individual cells, but also by the activation of these receptors in other neurons within a functional neural network in which $D_2$R activation affects the release of endocannabinoids or other modulators (Meschler et al. 2000). As such, we used electron microscopic immunolabeling to test the hypothesis that quinpirole elicits a region-specific in vivo change in the surface/synaptic availability of $D_2$ receptors in striatal neurons expressing the $CB_1$R 1 h following a single injection of 0.5 mg/kg quinpirole, a dose that suppressed locomotor activity in mice.

## Materials and methods

*Animals* The experimental procedures were carried out in accordance with the National Institutes of Health Guidelines for the Care and Use of Laboratory Animals, and approved by the Institutional Animal Care and Use Committees at Weill Medical College of Cornell University and the University of Washington. The locomotor activity of 12 adult male C57BL/6J mice (20–25 g; Jackson Laboratory, Bar Harbor, ME) was recorded in locomotor chambers (Med Associates, St. Albans, VT). These chambers consist of Plexiglass boxes with six infrared beam bars (1–2 on each side) positioned so as to measure both horizontal movement and rearing. The mice were habituated to the test chamber for 60 min 2 days prior to drug injection (day 1—habituation). The following consecutive day, baseline measures of locomotor activity were recorded (day 2—baseline measures). On the third consecutive day, animals received a subcutaneous injection of either quinpirole (0.5 mg/kg; $n$=6) or saline (control animals; $n$=6) and were immediately placed into the test chamber for 60 min, during which time locomotor activity was monitored (day 3—locomotor testing). Drug effects on locomotor activity were measured as ambulatory time and distance traveled. The data were evaluated using a repeated measure ANOVA. Immediately following the 60-min test period, the mice were deeply anesthetized by intraperitoneal injection of sodium pentobarbital (150 mg/kg) and brain tissue was fixed by vascular perfused with 30 ml of a solution containing 3.75% acrolein and 2.0% paraformaldehyde in 100 mM phosphate buffer, pH 7.4 (PB) followed by 150 ml of 2% paraformaldehyde in PB.

The acrolein-infused brains were removed from the cranium and post-fixed for 30 min in 2% paraformaldehyde in PB. Coronal sections of 40 μm were cut through the Acb and striatum (Franklin and Paxinos 1997) using a Leica

Vibratome (Leica Microsystems, Bannockburn, IL). The aldehyde-fixed tissue sections were collected in 0.1 MPB and then placed for 30 min in a solution of 1% sodium borohydride in 0.1 MPB to remove excess active aldehydes.

*Antisera* The full C terminus of the rat $CB_1R$ (Wager-Miller et al. 2002) was used to generate a polyclonal antiserum in guinea pig. This antiserum has been used previously for light microscopic immunolabeling in mouse brain (Mulder et al. 2008) where the immunoreactivity has a distribution pattern similar to that seen using an extensively characterized rabbit antiserum also directed against the $CB_1R$ C terminus (Katona et al. 1999; Katona et al. 2001). In the present study, we further tested the specificity of the guinea pig $CB_1R$ antiserum by comparison of the striatal labeling in wild-type and $CB_1R$ (−/−) mice.

A dopamine $D_2R$ antipeptide antiserum was generated in rabbit against amino acids 216–311 of the human $D_2R$ long isoform ($D_{2L}R$; Brana et al. 1997), which was cloned into the pET30c plasmid (Novagen, Madison, WI, USA) and confirmed by sequencing. The antiserum was affinity-purified and shown to be specific by positive immunolabeling in human embryonic kidney cells transiently transfected with the pcDNA-FLAG-D2L plasmid (Kearn et al. 2005). In Western blot analysis of rat brain homogenates, a single band at 50 kDa was recognized by the $D_{2L}R$ antiserum, and pre-adsorption with immobilized antigen eliminated the $D_2R$ immunoreactive band as well as the immunolabeling seen in sections through the rat forebrain (Pickel et al. 2006).

*Electron microscopic dual labeling* The dual-labeling protocol used for electron microscopy was modified from that originally described by Chan et al. (1990). For this, the prepared sections from the aldehyde-fixed tissue were incubated overnight at room temperature in a mixture of guinea pig anti-$CB_1R$ antiserum (1:1,000) and rabbit anti-$D_2R$ antiserum (1:250) in a solution of Tris–saline containing 0.1% bovine serum albumin.

For immunoperoxidase labeling of the guinea pig $CB_1R$ antiserum, sections previously incubated with both primary antisera were washed and placed for 30 min in biotinylated donkey anti-guinea pig immunoglobulin (IgG, 1:200; Jackson ImmunoResearch Laboratories, West Grove, PA, USA). These sections were then incubated for 30 min in Vectastain ABC Elite kit (Vector Laboratories, Burlingame, CA). The product was visualized by reaction in 3,3′-diaminobenzadine (Sigma-Aldrich, St. Louis, MO) and hydrogen peroxide. Subsequently, for immunogold labeling of the rabbit $D_2R$ antiserum, the tissue was washed and placed in a solution of Ultrasmall gold (Electron Microscopy Sciences, Hatfield, PA) conjugated to donkey anti-rabbit IgG. The particles were visualized by using the Silver IntensEM kit (GE Healthcare). The immunolabeled sections of tissue were post-fixed in 2% osmium tetroxide and embedded in plastic using conventional methods (Leranth et al. 1989).

*Electron microscopic data analysis* The regions of the ventromedial Acb shell and dorsolateral striatum in the atlas of (Franklin and Paxinos 1997) were chosen for ultrastructural analysis. A Leica ultramicrotome (Leica Microsystems, Wetzlar, Germany) was used to collect ultrathin sections from the surface of two immunolabeled sections from each of these regions in 12 mice (six receiving quinpirole and six saline). These thin sections were mounted on copper grids, counterstained using uranyl acetate and lead citrate (Reynolds 1963), and examined with a FEI Tecnai electron microscope (FEI, Hillsboro, OR). The thin sections were initially examined at low (8–9 K) magnification to identify the surface of the tissue, and those regions showing immunolabeling of both $CB_1$ and $D_2$ receptors. These were then magnified and captured as digital images. Thirty electron microscopic images at ×13,000 magnification were analyzed from the 24 blocks of tissue (2 sections from each of the 12 mice).

Immunoperoxidase labeling was regarded as positive when an electron dense precipitate, indicative of peroxidase reaction product, was seen in selective profiles but absent in adjacent profiles having otherwise similar ultrastructural features. Immunogold-labeled structures were identified as those containing one or more gold particles. This method was validated in immunogold-labeled tissue by ascertaining the absence of gold-silver deposits overlying myelin and other structures, not known to express either $D_2$ or $CB_1$ receptors.

The labeling patterns in Acb shell and dorsal striatum were quantitatively compared in thin sections taken from the surface of vibratome sections from each region. Electron microscopic images were obtained from a total tissue area of 41,616 $\mu m^2$, representing 10,404 $\mu m^2$ in each of four categories (CPu saline, CPu quinpirole, Acb saline, and Acb quinpirole). The immunolabeled structures were separated into categories of dendrites (dendritic shafts and spines), axon terminals, small neuronal profiles (mainly unmyelinated axons and spine necks), or glial processes according to the nomenclature of Peters et al. (1991). Labeled terminals were further defined with respect to the type of synaptic specialization and immunolabeling in the targeted neuron. Chi square, ANOVA, and paired *t* test analysis were done using JMP software (SAS Institute, Cary, NC). Figures were prepared from the acquired digital images by initial adjustment of contrast and brightness using Adobe Photoshop CS4 and Microsoft Office Excel and PowerPoint 2007 software.

## Results

Quinpirole suppressed locomotor activity throughout the 60 min interval following systemic injection (Fig. 1). One hour after injection, quinpirole also produced significant regional and compartment-specific changes in the subcellular distribution of $D_2$R-immunogold particles in somatodendritic and axonal profiles of mouse striatum. The $D_2$R containing profiles were largely without $CB_1$R immunoreactivity, a $CB_1$R-specific product seen by light microscopy in the striatum of wild-type, but not CB1R (−/−) mice (Fig. 2).

*Quinpirole-induced decrease in locomotor activity* Prior to quinpirole administration, there were no differences in baseline measures of locomotor activity, either in the ambulatory time or distance traveled, in mice used for the present study. However, after a single subcutaneous injection of quinpirole (0.5 mg/kg), mice showed a significant decrease in the amount of time they were active ($F$ (1, 20)=22.17, $p<0.05$) and in the distance they traveled ($F$(1, 20)=18.92, $p<0.05$) as compared with saline controls. Further, a repeated measures ANOVA showed that although all animals moved less across the 1 h time period (ambulatory time: ($F$(59, 1,180)=1.85, $p<0.05$; distance traveled: ($F$ (59, 1,180)= 1.77, $p<0.05$), there was no significant interaction between time and drug treatment (ambulatory time: ($F$ (177, 1,180)= 1.16, $p>0.05$); distance traveled: ($F$ (177, 1,180)=1.19, $p>0.05$). This suggests that the decrease in activity produced by

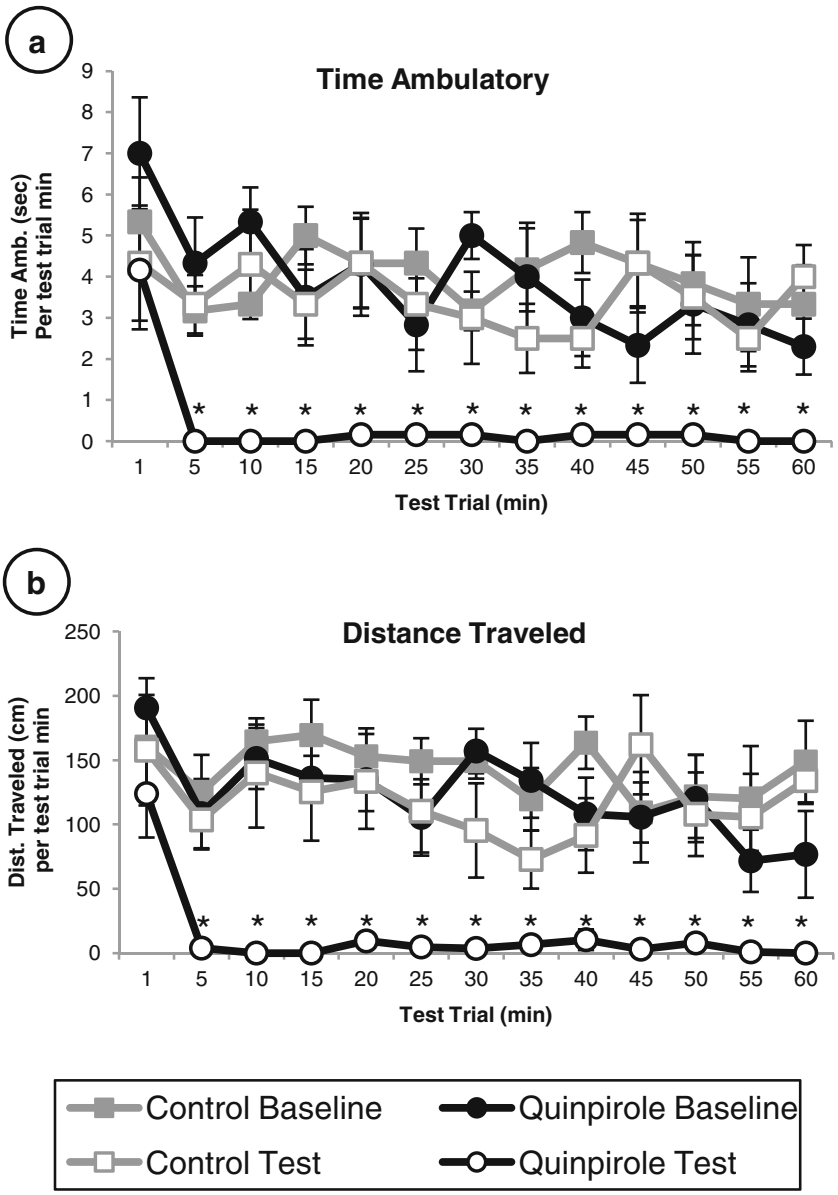


**Fig. 1** Line graphs showing locomotor activity in mice receiving a single subcutaneous injection (0.5 mg/kg) of the $D_2$/$D_3$ receptor agonist, quinpirole, or saline. Both ambulatory time (**a**) and distance traveled (**b**) are significantly reduced in the quinpirole treated (*open circle*) compared with saline-injected control (*open squares*) mice and with baseline measures of either treatment group (*filled circles and squares*). The quinpirole-induced reduction in activity is apparent within the first 5 min after injection and continues for the duration of the 1-h test period. Prior to quinpirole administration (baseline measures), mice show no significant differences in locomotor activity (*filled squares* indicate control mice, *filled circles* indicate quinpirole mice). Values are expressed as means and standard errors; $n$=6 animals/treatment group; *$p<0.05$

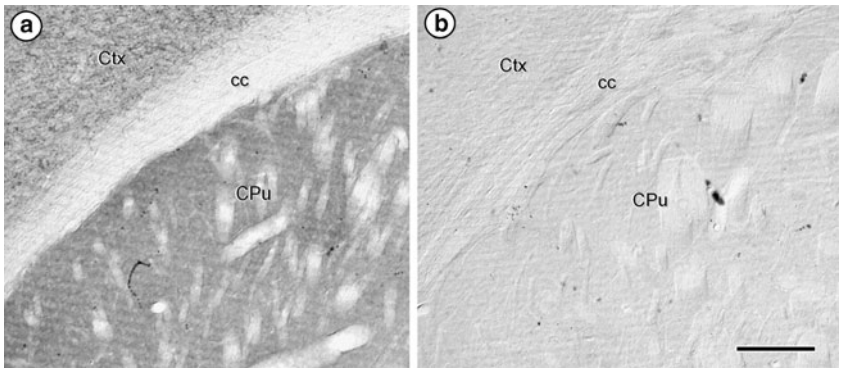


**Fig. 2** Light micrographs showing immunoperoxidase labeling for the guinea pig anti-$CB_1R$ antiserum in a coronal section through the dorsal striatum of a C57/BL6J wild-type (A), but not a $CB_1R$ (−/−) mouse. *c.c.* corpus callosum. *Scale bar*=100 μm

quinpirole is independent of the generally observed decrease in locomotor activity over time.

*Somatodendritic distribution and quinpirole-induced trafficking of $D_2Rs$* In both the Acb shell and dorsal striatum, $D_2R$ immunogold was discretely localized to the plasma membrane or associated with cytoplasmic endomembranes in somatodendritic profiles (Fig. 3). In somata, these endomembranes included smooth endoplasmic reticulum and Golgi lamellae near the nuclear membrane (Fig. 3a, b).

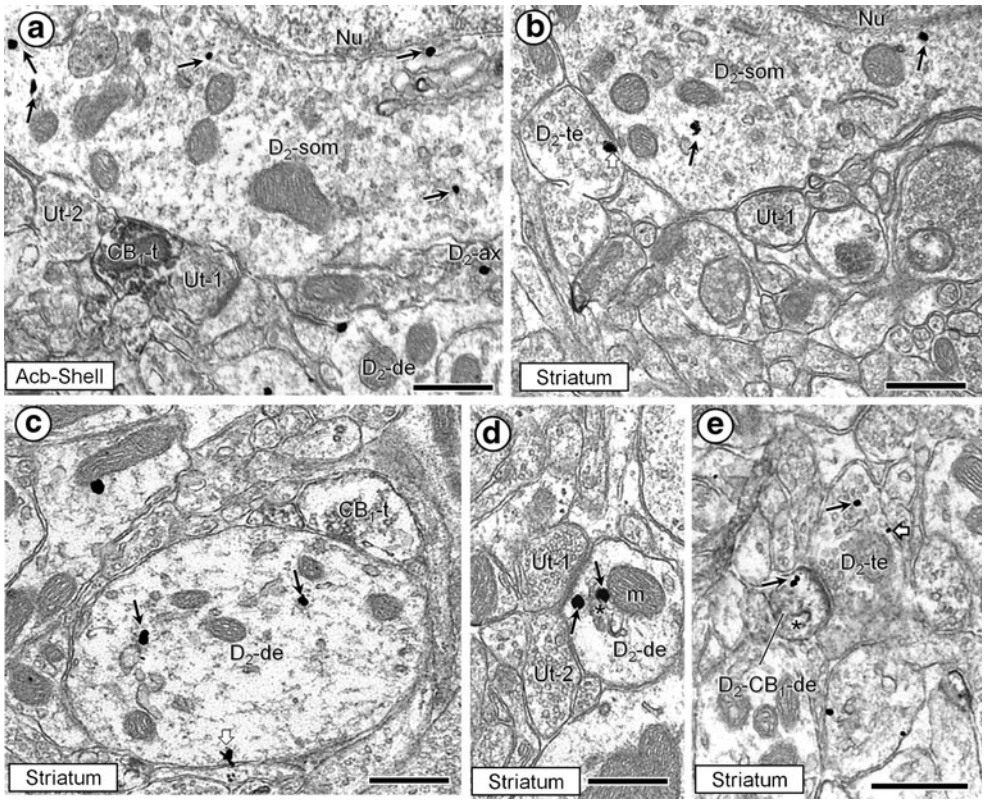


**Fig. 3** Electron micrographs showing $D_2R$ immunogold particles within the cytoplasm (*small black arrows*) and on the plasma membrane (*white block arrows*) of somatodendritic profiles without detectable $CB_1R$ immunoperoxidase labeling in the Acb shell (**a**) and dorsal striatum (G-D). In **a** and **b**, the somata are contacted by axonal profiles that are either unlabeled terminals (Ut-1–2), $CB_1R$ immunoperoxidase-labeled terminals ($CB_1$-t) or $D_2R$ containing axons ($D_2$-ax) or terminals ($D_2$-te). In **c**, immunogold particles identifying the $D_2R$ are seen in a transversely sectioned medium-diameter dendrite ($D_2$-de). This dendrite receives an inhibitory-type synapse from an axon terminal ($CB_1R$-t) showing faint $CB_1R$-immunoperoxidase labeling. In **d**, the cytoplasmic $D_2R$-immunogold particles are localized to endomembranes (*asterisk*) in the transition zone between the plasma membrane at an excitatory-type synapse and the outer membrane of a mitochondrion (**m**). Unlabeled terminals (Ut-1 and Ut-2) are presynaptic to the $D_2R$-labeled dendrite. In **e**, cytoplasmic immunogold labeling (*arrows*) for the $D_2R$ is seen in a small dendrite that also contains $CB_1R$-immunoperoxidase reaction product ($D_2$-$CB_1$-de) associated with an endomembrane (*asterisk*) and the postsynaptic membrane specialization beneath a $D_2R$-labeled axon terminal. Within this terminal, one immunogold particle is in the cytoplasm (*small black arrow*) and the second is in contact with the plasmalemma (*block arrow*). In bar graphs, values are expressed as means and standard errors; $n$=6 animals/treatment group; *$p$<0.05. In micrographs, *scale bars*=500 nm

$D_2R$-immunogold particles in dendrites and dendritic spines comprised more than half the total number of particles seen in the Acb shell or CPu (Table 1). As compared with somata, the $D_2R$-immunogold particles in dendrites were more frequently associated with the plasma membrane, but retained their predominant cytoplasmic endomembrane distribution (Fig. 3c, d). These endomembranes were often located near mitochondria, being most prevalent between the outer mitochondrial membrane and the postsynaptic membrane specialization of excitatory synapses (Fig. 3d). The immunoperoxidase labeling of the $CB_1R$ was also localized to endomembranes in dendrites, inclusive of those that contained $D_2R$ immunogold (Fig. 3e). The $D_2R$ and/or $CB_1R$-labeled dendrites received synaptic input from unlabeled terminals and from terminals containing either $CB_1R$ or $D_2R$, but rarely both receptors (Fig. 3). The synaptic contacts onto these dually labeled dendrites were not quantitatively examined, because of their small number. Only 12/3,715 of the $D_2R$-labeled dendrites and 8/1,205 of the D2R-labeled dendritic spines contained immunoperoxidase reaction product for the $CB_1R$.

Qualitative analysis of the $D_2R$-labeling in mice receiving quinpirole compared with saline suggested that quinpirole administration induced internalization of $D_2Rs$ in dendrites, the vast majority of which were without detectable $CB_1R$ immunoreactivity in the Acb shell (Fig. 4a, b). Quantitative analysis confirmed that in these dendrites quinpirole-induced a significant region-specific decrease in the plasmalemmal ($F(1, 1{,}808)=8.28$, $p<0.05$) and increase in the cytoplasmic ($F$ (1, 1,808)=7.37, $p<0.05$) density of $D_2R$-immunogold particles consistent with agonist-induced $D_2R$ internalization (Fig. 4c). No similar changes were seen in the dorsal striatum (Fig. 4d). Moreover, we saw no quantitative changes in the distribution of $D_2R$ within dendritic spines in Acb shell or striatum of mice with 1 h of quinpirole treatment (Data not shown).

*Axonal distribution and quinpirole-induced plasmalemmal enhancement of $D_2Rs$* In both the Acb shell and dorsal striatum, 33% of the $D_2R$-immunogold particles were located in axonal varicosities (Table 1). $D_2R$-immunogold particles were also located within small (<0.2 μm diameter) profiles in these regions, many of which had the ultrastructural l features of were small axons. Isolated $D_2R$-immunogold particles were discretely located in the cytoplasm overlying synaptic vesicles or in contact with the plasmalemma in the axonal varicosities of each region. These gold particles were also seen in many ($n$=991) small (<0.2 μm diameter) profiles having the morphological features of unmyelinated axons in the Acb shell and CPu of mice receiving either saline or quinpirole. The majority of the varicose axon terminals were without recognizable synaptic junctions, but they also formed asymmetric or more rarely symmetric synapses (Table 2), which are typical of axon terminals containing glutamate and GABA, respectively (Bellocchio et al. 1998; McDonald et al. 2002). The $D_2R$-labeled terminals forming asymmetric synapses contacted mainly unlabeled (Fig. 5a) or $D_2R$-labeled (Fig. 5b) dendritic spines; whereas those forming inhibitory-type synapses, principally contacted large dendrites (Fig. 5c) or somata (Fig. 5d, e). The $D_2R$-labeled axonal varicosities were substantially more abundant than those containing both $D_2R$ and $CB_1R$ immunoreactivity (Table 2). However, the dually labeled terminals were usually without recognizable synaptic membrane specializations within a single plane of section and were classified as undefined (Fig. 5d, e; Table 2).

In the Acb shell, the plasmalemmal associated $D_2R$-immunogold particles in axon terminals appeared to be slightly more prevalent in mice receiving quinpirole compared with saline (Fig. 5a, b). Quantitative analysis confirmed this impression and demonstrated a significantly higher plasmalemmal density of $D_2R$ immunogold in axon terminals without detectable $CB_1R$ immunoreactivity in the Acb shell ($F$ (1, 1186)=4.86. $p<0.05$; Fig. 6a). In the dorsal striatum of mice receiving quinpirole, there was also a significant ($F$ (1, 1,173)=3.96, $p<0.05$; Fig. 6b) increase in the plasmalemmal $D_2R$ immunogold in axon terminals, although this increase was not as readily apparent from qualitative observations. The quinpirole-induced plasma-

**Table 1** Percentage of $D_2R$-immunogold particles overlying dendritic and axonal profiles in the caudate nucleus and accumbens shell of mice receiving either saline or quinpirole

| | All groups | Caudate nucleus | | Accumbens shell | |
|---|---|---|---|---|---|
| | | Saline | Quinpirole | Saline | Quinpirole |
| Dendrites (%) | 54 | 53 | 55 | 54 | 54 |
| Dendritic spines (%) | 13 | 13 | 15 | 10 | 11 |
| Axonal varicosities (%) | 33 | 34 | 30 | 36 | 35 |
| Total[a] | 10,782 | 2,915 | 2,810 | 2,530 | 2,527 |

[a] $n$=total number of $D_2R$-immunogold particles in an area of 20,808 $\mu m^2$ tissue in the caudate nucleus and an equal area in the nucleus accumbens shell of 12 mice that received saline or quinpirole

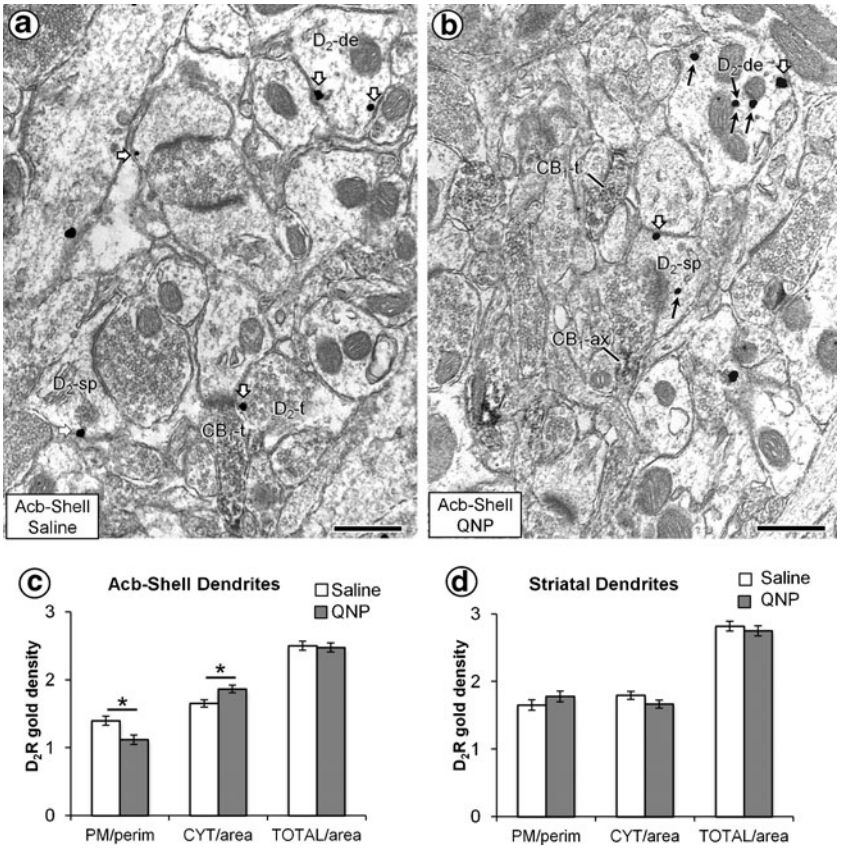


**Fig. 4** Quinpirole-induced shift in $D_2R$-immunogold particles from the plasma membrane (*block arrows*) to the cytoplasm (*small black arrows*) in dendritic profiles preferentially located in the Acb shell. Electron micrographs showing the immunogold silver $D_2R$ labeling in sections through the Acb shell of a mouse receiving saline (**a**) or quinpirole (QNP; **b** 1 h prior to sacrifice). In these micrographs, $CB_1R$-immunoperoxidase-labeled axon terminals ($CB_1$-t, $CB_1$-ax) form asymmetric excitatory-type synapses with dendritic spines, some of which show $D_2R$ immunogold ($D_2$-sp) as do nearby $D_2R$-immunogold-labeled terminals ($D_2$-t). **c** *Bar graphs* indicating that as compared with saline-injected controls, mice receiving quinpirole have a statistically significant (*asterisk*) reduction in plasmalemmal (number of particles per unit length; PM/perim) and an increase in cytoplasmic $D_2R$-immunogold density (number of particles per unit cytoplasmic area of the dendrite (CYT/area)). No between group differences are seen in the total (plasmalemmal and cytoplasmic) number of $D_2R$-immunogold particles per unit area (TOTAL/area) in dendrites of the Acb shell. **d** *Bar graphs* show no significant differences between quinpirole and saline treatment groups in the plasmalemmal, cytoplasmic, or total density of $D_2R$-immunogold particles in dendrites of the dorsal striatum. *Scale bars*=500 nm

lemmal increase in the density of $D_2R$-immunogold particles was accompanied by a small, non-significant increase in the cytoplasmic density of these particles in the Acb shell ($F$ (1, 1,186)=0.78, $p>0.05$). This increase in cytoplasmic density may have contributed to the significant increase in the total (plasmalemmal and cytoplasmic)

**Table 2** Percentage distribution of dendritic contacts formed by single ($D_2R$) and dual ($D_2R$+$CB_1R$)-labeled axonal varicosities in the mouse caudate nucleus and accumbens (Acb) shell

| Caudate nucleus | | | Nucleus accumbens shell | |
|---|---|---|---|---|
| Contact | $D_2R$ terminals | $D_2R$ + $CB_1R$ terminals | $D_2R$ terminals | D2R + CB1R terminals |
| Asymmetric (%) | 40 | 9 | 36 | 17 |
| Symmetric (%) | 4 | 15 | 10 | 19 |
| Undefined (%) | 56 | 76 | 54 | 64 |
| Total[a] | 1,173 | 132 | 1,186 | 110 |

[a] $n$=number of labeled varicosities seen in an area of 20,808 $\mu m^2$ in the caudate nucleus and an equal area in the accumbens shell of 12 mice that received either saline or quinpirole

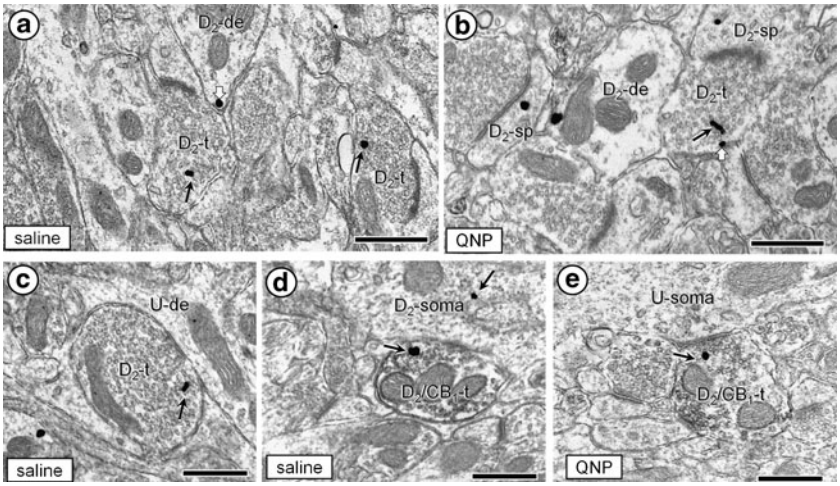


**Fig. 5** Electron micrographs showing $D_2$R-immunogold labeling in axon terminals ($D_2$-t) within the Acb shell of mice having 1 h previously received quinpirole (QNP) or saline. Images in **a** and **b** provide qualitative evidence for increased plasmalemmal (*white block arrows*) $D_2$R-immunogold labeling in axon terminals ($D_2$-t) forming asymmetric, excitatory-type synapses with dendritic spines. These terminals are without detectable $CB_1$R-immunoperoxidase labeling, as is the terminal in **c** which forms a symmetric synapses with and unlabeled dendrite (U-de). In contrast, the inhibitory-type terminals ($D_2$/$CB_1$-t) seen in **d** and **e** contain both $D_2$R-immunogold and $CB_1$R-immunoperoxidase labeling with no apparent treatment-specific differences in the plasmalemmal $D_2$R distribution. The dually labeled terminal forms a synapses with a $D_2$R-labeled soma ($D_2$-soma) in **d** and an unlabeled soma (U-soma) in **e**. *Small black arrows* indicate cytoplasmic and block arrows indicate plasmalemmal $D_2$R-immunogold particles. *Microscopic scale bars*=500 nm

density of $D_2$R-immunogold particles in terminals of this region when they expressed $D_2$R alone ($F$ (1, 1,186)=6.40, $p$<0.05; Fig. 6a) but not together with the $CB_1$R ($F$ (1, 110)= 1.6, $p$>0.05; Fig. 6c). Dual-labeled terminals in the dorsal striatum (Fig. 6d) also failed to show a change in the total (plasmalemmal and cytoplasmic) density of $D_2$R

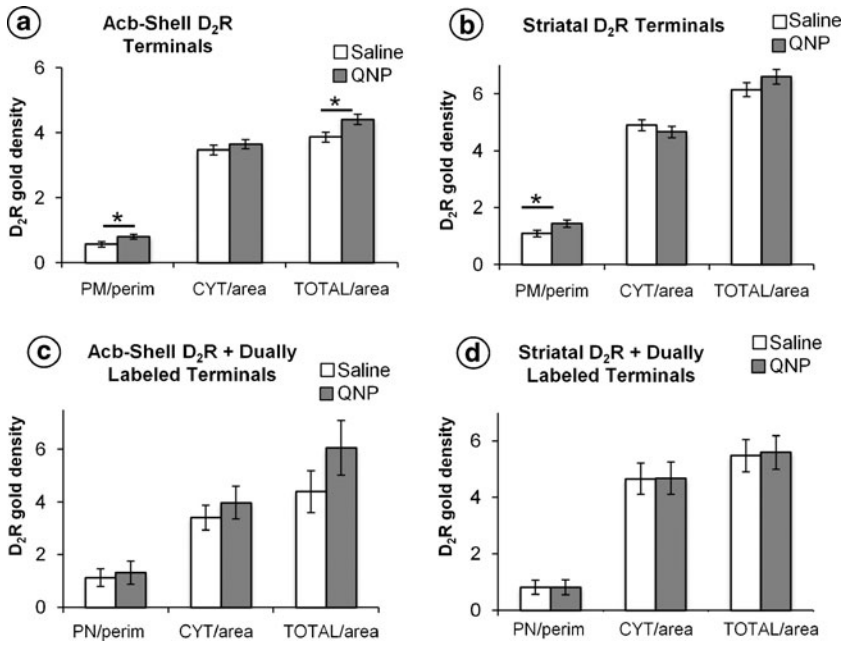


**Fig. 6** *Bar graphs* showing that $D_2$R-immunogold particles in axon terminals without $CB_1$R labeling have a significantly greater plasmalemmal density, number/length axonal plasma membrane or, perimeter (PM/perim) in the Acb shell (**a**) and striatum (**b**) of mice receiving quinpirole (QNP) compared with saline. In the Acb shell of mice receiving quinpirole, there is also a significant increase above the saline controls in the total density (cytoplasmic + plasmalemmal) of $D_2$R-immunogold particles in axon terminals. Neither the plasmalemmal, cytoplasmic, nor total densities of $D_2$R-immunogold particles in dually labeled terminals in the Acb shell or dorsal striatum (**c** and **d**) significantly differ between quinpirole and saline-injected mice. Values are expressed as means and standard errors; $n$=6 animals/treatment group; *$p$<0.05

immunogold in mice receiving quinpirole ($F$ (1,132)=0.02, $p$>0.05).

## Discussion

Our results provide in vivo evidence for region-specific trafficking of $D_2$Rs in dendritic and axonal compartment without detectable $CB_1$R labeling in mouse striatum at 1 h following systemic administration of quinpirole. The preferential quinpirole-induced plasmalemmal to cytoplasmic redistribution of $D_2$R-immunogold particles in dendrites of the Acb shell suggests that postsynaptic neurons in this region show agonist-induced $D_2$R internalization that is detectable at 1 h following drug administration. At this time point, however, we observed an increase in the plasmalemmal density of $D_2$R immunogold in axonal varicosities in both the Acb shell and CPu of mice receiving quinpirole compared with saline. This suggests that the agonist-induced internalization of D2Rs seen in dendrites either does not occur or is followed by a more rapid surface replenishment in striatal axon terminals. The quinpirole-induced changes in the pre- and/or postsynaptic surface availability of $D_2$Rs particularly in the Acb shell may result in disinhibition of output neurons in the ventral pallidum mediating, in part, the suppression of locomotor activity (Hooks and Kalivas 1995; Nicola 2007; Sesack and Grace 2010) as is hypothetically diagramed in Fig. 7. These findings demonstrate network-dependent changes in $D_2$R trafficking following activation, which would be difficult to discern outside the context of an intact, functional system.

*Trafficking of $D_2$Rs in dendrites* The observed decrease in plasmalemmal and increase in cytoplasmic density of $D_2$R immunogold in postsynaptic dendrites of the Acb shell 1 h following quinpirole administration suggests that the $D_2$Rs are being internalized to cytoplasmic compartments where they are retained in a form recognizable by the $D_2$R antiserum. Cytoplasmic $D_2$R immunogold in somata and dendrites was often associated with endomembranes that are involved in the dynamic transport of proteins in both directions along dendritic microtubules(Gruenberg et al. 1989; Prekeris et al. 1998). The identity of these membranes as portions of endomembrane systems associated with the trafficking of G protein-coupled receptors is suggested by their resemblance to early endosomes, where the receptors are dephosphorylated and either retained or recycled back to the cell surface (Seachrist and Ferguson 2003).

Few of the dendritic segments expressing $D_2$Rs contained $CB_1$R labeling in mouse Acb shell or CPu, even though these receptors are often co-expressed in these regions of rat brain (Ong and Mackie 1999; Pickel et al.

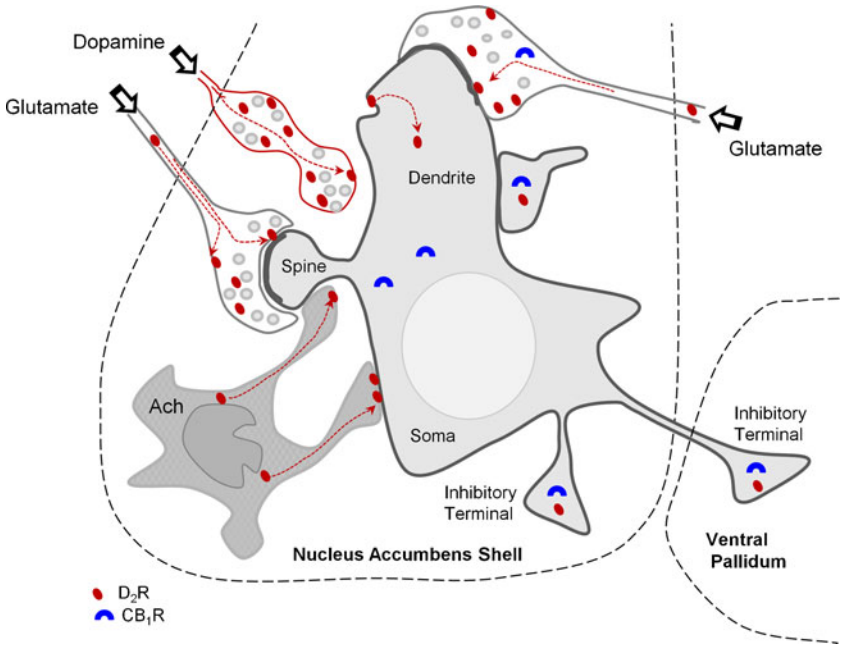


**Fig. 7** Simplified schematic diagram showing the hypothesized quinpirole-induced $D_2$R mobilization (*dashed arrows*) from the plasma membrane to the cytoplasm in a postsynaptic dendrite. *Block arrows* indicate extrinsic glutamatergic and dopaminergic inputs. An intrinsic (cholinergic interneurons, Ach) somata is also shown to provide input to a medium spiny neuron in the Acb shell. This spiny neuron is shown as giving rise to local and extrinsic (ventral pallidum) inhibitory-type terminals expressing both the $D_2$R and $CB_1$R. Within this framework, locomotor inhibition would result from the heightened $D_2$R-mediated inhibition of the release of stimulatory transmitters (glutamate and/or acetylcholine) onto a motor-activating spiny projection neuron, whose activity is further suppressed by agonist-induced activation of postsynaptic $D_2$Rs

2006). The infrequent detection of $CB_1R$ immunoreactivity in $D_2R$-containing dendrites of mouse striatum may have resulted in an underestimation of the dendritic co-expression of these receptors in the present study. However, this would not be expected to affect our comparison of the location of $D_2Rs$ in quinpirole- versus saline-injected mice, since both treatment groups would be subject to the same limitation.

*$CB_1R$ expression in presynaptic terminals apposing $D_2R$-labeled dendrites* In contrast with the low abundance of $CB_1R$ immunoreactivity in $D_2R$-containing dendrites, the $CB_1R$ was prevalent in axon terminals providing synaptic input to these dendrites. The respective location of $D_2$ and $CB_1$ receptors in dendrites and their afferent terminals, many of which form asymmetric excitatory-type synapses, supports prior evidence that activation of postsynaptic $D_2Rs$ contributes to the mobilization of endocannabinoids that suppress glutamate release through activation of presynaptic $CB_1$ receptors (Eilam and Szechtman 1989). More excitatory-type terminals contain $CB_1$ receptors in the Acb shell compared with the core (Pickel et al. 2004), a region that receives less extensive glutamatergic input from the prefrontal cortex and shows both structural and functional similarity to the CPu (Zahm 2000). Thus, our detection of dendritic trafficking of the $D_2R$ receptor in the Acb shell, but not the CPu, may reflect in part a more substantial $D_2R$-mediated change in endocannabinoid signaling affecting the presynaptic release of glutamate from prefrontal cortical inputs to the Acb shell (Robbe et al. 2002).

*Increased presynaptic plasmalemmal density of $D_2Rs$* We observed an increase in plasmalemmal density of the $D_2R$ with (Acb shell) or without (dorsal striatum) a concomitant increase in the cytoplasmic density of these receptors in axon terminals at 60 min following quinpirole administration. Our observations support the in vitro evidence that quinpirole elicits an accumulation of $D_2R$/sGi2, a spliced variant of the GTP-binding protein G(alpha i2), in neurites and membranes (Tirotta et al. 2008). This effect may be secondary to the activation and internalization of $D_2Rs$, which can occur within as little as 20 min following quinpirole administration (Kita et al. 2007). Thus, at 1 h following systemic administration of quinpirole, the internalized $D_2Rs$ may be already returned to the plasmalemmal surface where newly recruited receptors are also accumulated. The structural diversity of the $D_2R$-containing axonal profiles included among those showing a quinpirole-induced enhancement of plasmalemmal $D_2Rs$ suggests that they arise from extrinsic as well as local striatal neurons.

The axon terminals showing quinpirole-induced up-regulation of plasmalemmal $D_2Rs$ include the many varicosities without clearly defined synaptic specializations, a feature that is typical of dopaminergic inputs to both the dorsal and ventral striatum (Nirenberg et al. 1997; Pickel et al. 1997). Presynaptic $D_2$ autoreceptors are prevalent throughout the striatum, where low doses of quinpirole are highly effective in producing calcium-dependent inhibition of the spontaneous release of dopamine (Garcia-Sanz et al. 2001). Although endocannabinoids can modulate $D_2R$-mediated inhibition of dopamine release (O'Neill et al. 2009), there is to our knowledge no evidence that the $CB_1R$ is present in dopaminergic terminals.

Of the $D_2R$-labeled terminals forming synapses in the Acb shell and CPu, the majority were characterized by asymmetric, excitatory-type junctions typical of glutamatergic neurons (Charara et al. 1996; Torrealba and Müller 1999). A quinpirole-induced increase in the plasmalemmal expression of $D_2Rs$ in these terminals within the Acb shell is consistent with the fact that local injection of quinpirole in this region decreases locomotor exploration, an effect ascribed to $D_2R$-dependent inhibition of glutamate release (Kalivas and Duffy 1997; Mogenson and Wu 1991). A quinpirole-induced increase in the presynaptic availability of $D_2Rs$ in glutamatergic terminals might make these terminals more susceptible to $D_2R$-mediated inhibition of glutamate release thus accounting for the functional synergy between quinpirole and glutamate NMDA receptor antagonists (Bortolato et al. 2005).

The relatively small number of $D_2R$-labeled terminals that formed symmetric inhibitory-type synapses in either the Acb shell or CPu may reflect in part their inclusion in the category of non-synaptic synapses because of the difficulty in recognizing the thin pre- and postsynaptic membrane specializations that are typical of GABAergic neurons (Oertel and Mugnaini 1984; Pickel and Heras 1996; Smith et al. 1987). That the inhibitory-type terminals containing $D_2R$ as well as the $D_2R$ and $CB_1R$ labeling may have been underestimation in the mouse Acb shell and CPu of the present study is suggested by our prior demonstration that in these terminals are prevalent within these regions in rat striatum (Pickel et al. 2006). However, the species difference may also account for these observations in $D_2R$ labeling in these terminals.

In contrast to axon terminals without $CB_1R$ immunolabeling, the subcellular distribution of $D_2Rs$ within dual-labeled terminals did not significantly differ from saline-injected controls. Systemic administration of quinpirole produces an up-regulation of endocannabinoid signaling (Giuffrida et al. 1999; Swanson et al. 1997; van der Stelt and Di 2003; Van Hartesveldt 1997). Individually, $D_2$ and $CB_1$ receptors are coupled to inhibitory G-proteins ($G_i$; Bouaboula et al. 1999; Jarrahian et al. 2004). When co-expressed, however, the dual activation of these receptors results in the formation of $D_2/CB_1$ heterodimers linked to stimulatory G-proteins ($G_s$; Glass and Felder, 1997; Kearn

et al. 2005; Pickel et al. 2006; Przybyla and Watts 2010). Thus, the quinpirole-induced increase in plasmalemmal $D_2$Rs in axonal profiles may greatly enhance the $D_2$R-mediated inhibition of the release of neurotransmitters from terminals that may also be subject to altered retrograde endocannabinoid signaling (Patel et al. 2003). Further, the formation of heterodimers when $D_2$ and $CB_1$ receptors are co-expressed in inhibitory-type terminals may change receptor dynamics providing a rationale for the lack of significant plasmalemmal trafficking of $D_2$Rs as seen in profiles lacking $CB_1$R labeling.

## Conclusion

Our findings show that systemic quinpirole administration produces region-specific and opposing changes in the dendritic and axonal distributions of $D_2$Rs which function collectively to decrease striatal dopamine signaling. First, quinpirole increased cytoplasmic $D_2$R labeling in dendrites within the Acb shell, whose neurons send extensive inhibitory projections to the ventral pallidum, a critical component in the neural network that normally has a permissive role in locomotor activity (Churchill et al. 1992; Kalivas et al. 1993; Murer et al. 2000). The quinpirole-induced internalization of $D_2$Rs in these cells, most likely, contributed to the observed decrease in locomotor activity. Second, there was increased plasmalemmal $D_2$Rs in axonal varicosities in the Acb shell and CPu. The greater availability of presynaptic $D_2$Rs on the plasma membrane in these regions may significantly increase $D_2$R-mediated inhibition of the release of dopamine and other transmitters that control motivational and sensorimotor activities through the output circuitry of the basal ganglia (Balleine et al. 2007; Belin et al. 2009). Finally, in contrast to $D_2$R single labeled profiles, axons containing $CB_1$Rs did not show significant plasmalemmal trafficking of $D_2$Rs possibly due to endocannabinoid mediated changes in receptor dynamics. Together, our findings reveal quinpirole-induced changes in the distribution of $D_2$Rs that might not be expected from agonist-induced internalization and trafficking seen in vitro. This demonstrates the importance of studying intact neural systems for understanding the consequences of agonist activation on the availability of functional surface receptors.

**Acknowledgments** This work was supported with grants from NIH: MH40342; DA04600 and DA005130 to VMP and DA011322 and DA021696 to KM.



## References

Artigas F (2010) The prefrontal cortex: a target for antipsychotic drugs. Acta Psychiatr Scand 121:11–21

Balleine B, Delgado M, Hikosaka O (2007) The role of the dorsal striatum in reward and decision-making. Journal of Neuroscience 27:8161-8165

Bamford NS, Zhang H, Schmitz Y, Wu NP, Cepeda C, Levine MS, Schmauss C, Zakharenko SS, Zablow L, Sulzer D (2004) Heterosynaptic dopamine neurotransmission selects sets of corticostriatal terminals. Neuron 42:653–663

Belin D, Jonkman S, Dickinson A, Robbins TW, Everitt BJ (2009) Parallel and interactive learning processes within the basal ganglia: relevance for the understanding of addiction. Behav Brain Res 199:89-102

Bellocchio E, Hu H, Pohorille A, Chan J, Pickel V, Edwards R (1998) The localization of the brain-specific inorganic phosphate transporter suggests a specific presynaptic role in glutamatergic transmission. J Neurosci 18:8648–8659

Besson M, Belin D, McNamara R, Theobald D, Castel A, Beckett V, Crittenden B, Newman A, Everitt B, Robbins T, Dalley J (2010) Dissociable control of impulsivity in rats by dopamine d2/3 receptors in the core and shell subregions of the nucleus accumbens. Neuropsychopharmacology 35:560–569

Bortolato M, Aru G, Fa M, Frau R, Orru M, Salis P, Casti A, Luckey G, Mereu G, Gessa G (2005) Activation of D1, but not D2 receptors potentiates dizocilpine-mediated disruption of prepulse inhibition of the startle. Neuropsychopharmacology 30:561–574

Bouaboula M, Bianchini L, McKenzie F, Pouyssegur J, Casellas P (1999) Cannabinoid receptor CB1 activates the Na+/H+ exchanger NHE-1 isoform via Gi-mediated mitogen activated protein kinase signaling transduction pathways. FEBS Lett 449:61–65

Brana C, Aubert I, Charron G, Pellevoisin C, Bloch B (1997) Ontogeny of the striatal neurons expressing the D2 dopamine receptor in humans: an in situ hybridization and receptor-binding study. Mol Brain Res 48:389–400

Chan J, Aoki C, Pickel V (1990) Optimization of differential immunogold-silver and peroxidase labeling with maintenance of ultrastructure in brain sections before plastic embedding. J Neurosci Methods 33:113–127

Charara A, Smith Y, Parent A (1996) Glutamatergic inputs from the pedunculopontine nucleus to midbrain dopaminergic neurons in primates: phaseolus vulgaris-leucoagglutinin anterograde labeling combined with postembedding glutamate and GABA immunohistochemistry. J Comp Neurol 364:254–266

Churchill L, Austin MC, Kalivas PW (1992) Dopamine and endogenous opioid regulation of picrotoxin-induced locomotion in the ventral pallidum after dopamine depletion in the nucleus accumbens. Psychopharmacology (Berl) 108:141–146

Del Arco A, Mora F (2009) Neurotransmitters and prefrontal cortex-limbic system interactions: implications for plasticity and psychiatric disorders. J Neural Transm 116:941–952

Delle Donne KT, Sesack SR, Pickel VM (1997) Ultrastructural immunocytochemical localization of the dopamine D2 receptor within GABAergic neurons of the rat striatum. Brain Res 746:239–255

Durstewitz D, Seamans J, Sejnowski T (2000) Dopamine-mediated stabilization of delay-period activity in a network model of prefrontal cortex. J Neurophysiol 83:1733–1750

Eilam D, Szechtman H (1989) Biphasic effect of D-2 agonist quinpirole on locomotion and movements. Eur J Pharmacol 161:151–157

Franklin K, Paxinos G (1997) The mouse brain in stereotaxic coordinates. Academic, San Diego

Garcia-Sanz A, Badia A, Clos M (2001) Differential effect of quinpirole and 7-OH-DPAT on the spontaneous [(3)H]-dopamine efflux from rat striatal synaptosomes. Synapse 40:65–73

Giuffrida A, Parsons L, Kerr T, Rodriguez dF, Navarro M, Piomelli D (1999) Dopamine activation of endogenous cannabinoid signaling in dorsal striatum. Nat Neurosci 2:358–363

Glass M, Felder C (1997) Concurrent stimulation of cannabinoid CB1 and dopamine D2 receptors augments cAMP accumulation in striatal neurons: evidence for a Gs linkage to the CB1 receptor. J of Neurosci 17:5327–5333

Gorriti MA, Ferrer B, del Arco I, Bermudez-Silva FJ, de Diego Y, Fernandez-Espejo E, Navarro M, Rodriguez de Fonseca F (2005) Acute delta9-tetrahydrocannabinol exposure facilitates quinpirole-induced hyperlocomotion. Pharmacol Biochem Behav 81:71–77

Gruenberg J, Griffiths G, Howell K (1989) Characterization of the early endosome and putative endocytic carrier vesicles in vivo and with an assay of vesicle fusion in vitro. J Cell Biol 108:1301–1316

Hersch SM, Yi H, Heilman CJ, Edwards RH, Levey AI (1997) Subcellular localization and molecular topology of the dopamine transporter in the striatum and substantia nigra. J Comp Neurol 388:211–227

Hooks M, Kalivas P (1995) The role of mesoaccumbens–pallidal circuitry in novelty-induced behavioral activation. Neurosci 64:587–597

Ikemoto S (2002) Ventral striatal anatomy of locomotor activity induced by cocaine, D-amphetamine, dopamine and D1/D2 agonists. Neuroscience 113:939–955

Jarrahian A, Watts VJ, Barker EL (2004) D2 dopamine receptors modulate Galpha-subunit coupling of the CB1 cannabinoid receptor. J Pharmacol Exp Ther 308:880–886

Kalivas PW, Duffy P (1997) Dopamine regulation of extracellular glutamate in the nucleus accumbens. Brain Res 761:173–177

Kalivas P, Churchill L, Klitenick M (1993) GABA and enkephalin projection from the nucleus accumbens and ventral pallidum to the ventral tegmental area. Neurosci 57:1047–1060

Katona I, Rancz E, Acsady L, Ledent C, Mackie K, Hajos N, Freund T (2001) Distribution of CB1 cannabinoid receptors in the amygdala and their role in the control of GABAergic transmission. J Neurosci 21:9506–9518

Katona I, Sperlagh B, Sik A, Kafalvi A, Vizi E, Mackie K, Freund T (1999) Presynaptically located CB1 cannabinoid receptors regulate GABA release from axon terminals of specific hippocampal interneurons. J Neurosci 19:4544–4558

Kearn C, Blake-Palmer K, Daniel E, Mackie K, Glass M (2005) Concurrent stimulation of cannabinoid CB1 and dopamine D2 receptors enhances heterodimer formation: a mechanism for receptor cross-talk? Mol Pharmacol 67:1697–1704

Kienast T, Heinz A (2006) Dopamine and the diseased brain. CNS Neurol Disord Drug Targets 5:109–131

Kim O, Ariano M, Namkung Y, Marinec P, Kim E, Han J, Sibley D (2008) D2 dopamine receptor expression and trafficking is regulated through direct interactions with ZIP. J Neurochem 106:83–95

Kita J, Parker L, Phillips P, Garris P, Wightman R (2007) Paradoxical modulation of short-term facilitation of dopamine release by dopamine autoreceptors. J Neurochem 102:1115–1124

Lee B, London ED, Poldrack RA, Farahi J, Nacca A, Monterosso JR, Mumford JA, Bokarius AV, Dahlbom M, Mukherjee J, Bilder RM, Brody AL, Mandelkern MA (2009) Striatal dopamine d2/d3 receptor availability is reduced in methamphetamine dependence and is linked to impulsivity. J Neurosci 29:14734–14740

Leranth C, Pickel V, Heimer L, Zaborszky L (1989) Electron microscopic pre-embedding double immunostaining methods Neuroanatomical Tract-tracing Methods 2: Recent Progress. Plenum Publishing Co., New York, pp 129–172

Martin AB, Fernandez-Espejo E, Ferrer B, Gorriti MA, Bilbao A, Navarro M, Rodriguez de Fonseca F, Moratalla R (2008) Expression and function of CB1 receptor in the rat striatum: localization and effects on D1 and D2 dopamine receptor-mediated motor behaviors. Neuropsychopharmacol 33:1667–1679

McDonald AJ, Muller JF, Mascagni F (2002) GABAergic innervation of alpha type II calcium/calmodulin-dependent protein kinase immunoreactive pyramidal neurons in the rat basolateral amygdala. J Comp Neurol 446:199–218

Meschler J, Conley T, Howlett A (2000) Cannabinoid and dopamine interaction in rodent brain: effects on locomotor activity. Pharmacol Biochem Behav 67:567–573

Missale C, Nash S, Robinson S, Jaber M, Caron M (1998) Dopamine receptors: from structure to function. Physiol Rev 78:189–225

Mogenson G, Wu M (1991) Effects of administration of dopamine D2 agonist quinpirole on exploratory locomotion. Brain Res 551:216–220

Mulder J, Aguado T, Keimpema E, Barabas K, Ballester Rosado CJ, Nguyen L, Monory K, Marsicano G, Di Marzo V, Hurd YL, Guillemot F, Mackie K, Lutz B, Guzman M, Lu HC, Galve-Roperh I, Harkany T (2008) Endocannabinoid signaling controls pyramidal cell specification and long-range axon patterning. Proc Natl Acad Sci USA 105:8760–8765

Murer M, Dziewczapolski G, Salin P, Vila M, Tseng K, Ruberg M, Rubinstein M, Kelly M, Grandy D, Low M, Hirsch E, Raisman-Vozari R, Gershanik O (2000) The indirect basal ganglia pathway in dopamine D(2) receptor-deficient mice. Neuroscience 99:643–650

Namkung Y, Dipace C, Javitch JA, Sibley DR (2009) G protein-coupled receptor kinase-mediated phosphorylation regulates post-endocytic trafficking of the D2 dopamine receptor. J Biol Chem 284:15038–15051

Nicola S (2007) The nucleus accumbens as part of a basal ganglia action selection circuit. Psychopharmacology (Berl) 191:521–550

Nirenberg M, Chan J, Pohorille A, Vaughan R, Uhl G, Kuhar M, Pickel V (1997) The dopamine transporter: comparative ultrastructure of dopaminergic axons in limbic and motor compartments of the nucleus accumbens. J Neurosci 17:6899–6907

Noble E (2003) D2 dopamine receptor gene in psychiatric and neurologic disorders and its phenotypes. Am J Med Genet 116B:103–125

O'Neill C, Evers-Donnelly A, Nicholson D, O'Boyle KM, O'Connor JJ (2009) D2 receptor-mediated inhibition of dopamine release in the rat striatum in vitro is modulated by CB1 receptors: studies using fast cyclic voltammetry. J Neurochem 108:545–551

Oertel W, Mugnaini E (1984) Immunocytochemical studies of GABAergic neurons in rat basal ganglia and their relations to other neuronal systems. Neurosci Lett 47:233–238

Ong W, Mackie K (1999) A light and electron microscopic study of the CB1 cannabinoid receptor in the primate spinal cord. J Neurocytol 28:39–45

Patel S, Rademacher D, Hillard C (2003) Differential regulation of the endocannabinoids anandamide and 2-arachidonylglycerol within the limbic forebrain by dopamine receptor activity. J Pharmacol Exp Ther 306:880–888

Peters A, Palay S, Webster H (1991) The fine structure of the nervous system. Oxford University Press, New York

Pickel V, Chan J, Kash T, Rodriguez J, Mackie K (2004) Compartment-specific localization of cannabinoid 1 (CB1) and [mu]-opioid receptors in rat nucleus accumbens. Neuroscience 127:101–112

Pickel V, Chan J, Kearn C, Mackie K (2006) Targeting dopamine D2 and cannabinoid-1 (CB1) receptors in rat nucleus accumbens. J Comp Neurol 495:299–313

Pickel V, Heras A (1996) Ultrastructural localization of calbindin-D 28 k and GABA in the matrix compartment of the rat caudate-putamen nuclei. Neuroscience 71:167–178

Pickel V, Nirenberg M, Milner T (1997) Ultrastructural view of central catecholaminergic transmission: immunocytochemical localization of synthesizing enzymes, transporters and receptors. J Neurocytol 25:843–856

Prekeris R, Klumperman J, Chen Y, Scheller R (1998) Syntaxin 13 mediates cycling of plasma membrane proteins via tubulovesicular recycling endosomes. J Cell Biol 143:957–971

Przybyla JA, Watts VJ (2010) Ligand-induced regulation and localization of cannabinoid CB1 and dopamine D2L receptor heterodimers. J Pharmacol Exp Ther 332:710–719

Reynolds E (1963) The use of lead citrate at high pH as an electron-opaque stain in electron microscopy. J Cell Biol 17:208–212

Robbe D, Kopf M, Remaury A, Bockaert J, Manzoni O (2002) Endogenous cannabinoids mediate long-term synaptic depression in the nucleus accumbens. Proc Natl Acad Sci USA 99:8384–8388

Schlagenhauf F, Juckel G, Koslowski M, Kahnt T, Knutson B, Dembler T, Kienast T, Gallinat J, Wrase J, Heinz A (2008) Reward system activation in schizophrenic patients switched from typical neuroleptics to olanzapine. Psychopharmacology (Berl) 196:673–684

Seachrist J, Ferguson S (2003) Regulation of G protein-coupled receptor endocytosis and trafficking by Rab GTPases. Life Sci 74:225–235

Sesack S, Grace A (2010) Cortico-Basal Ganglia reward network: microcircuitry. Neuropsychopharmacology 35:27–47

Skinbjerg M, Liow JS, Seneca N, Hong J, Lu S, Thorsell A, Heilig M, Pike VW, Halldin C, Sibley DR, Innis RB (2010) D2 dopamine receptor internalization prolongs the decrease of radioligand binding after amphetamine: a PET study in a receptor internalization-deficient mouse model. NeuroImage 50:1402–1407

Smith Y, Parent A, Seguela P, Descarries L (1987) Distribution of GABA-immunoreactive neurons in the basal ganglia of the squirrel monkey (Saimiri sciureus). J Comp Neurol 259:50–64

Soiza-Reilly M, Azcurra J (2009) Developmental striatal critical period of activity-dependent plasticity is also a window of susceptibility for haloperidol induced adult motor alterations. Neurotoxicol Teratol 31:191–197

Swanson C, Heath S, Stratford T, Kelley A (1997) Differential behavioral responses to dopaminergic stimulation of nucleus accumbens subregions in the rat. Pharmacol Biochem Behav 58:933–945

Tirotta E, Fontaine V, Picetti R, Lombardi M, Samad T, Oulad-Abdelghani M, Edwards R, Borrelli E (2008) Signaling by dopamine regulates D2 receptors trafficking at the membrane. Cell Cycle 7:2241–2248

Torrealba F, Müller C (1999) Ultrastructure of glutamate and GABA immunoreactive axon terminals of the rat nucleus tractus solitarius, with a note on infralimbic cortex afferents. Brain Res 820:20–30

van der Stelt M, Di MV (2003) The endocannabinoid system in the basal ganglia and in the mesolimbic reward system: implications for neurological and psychiatric disorders. Eur J Pharmacol 480:133–150

Van Hartesveldt C (1997) Temporal and environmental effects on quinpirole-induced biphasic locomotion in rats. Pharmacol Biochem Behav 58:955–960

Van Hartesveldt C, Cottrell GA, Potter T, Meyer ME (1992) Effects of intracerebral quinpirole on locomotion in rats. Eur J Pharmacol 214:27–32

Wager-Miller J, Westenbroek R, Mackie K (2002) Dimerization of G protein-coupled receptors: CB1 cannabinoid receptors as an example. Chem Phys Lipids 121:83–89

Wang Z, Kai L, Day M, Ronesi J, Yin H, Ding J, Tkatch T, Lovinger D, Surmeier D (2006) Dopaminergic control of corticostriatal long-term synaptic depression in medium spiny neurons is mediated by cholinergic interneurons. Neuron 50:443–452

Xiao MF, Xu JC, Tereshchenko Y, Novak D, Schachner M, Kleene R (2009) Neural cell adhesion molecule modulates dopaminergic signaling and behavior by regulating dopamine D2 receptor internalization. J Neurosci 29:14752–14763

Yao W, Spealman R, Zhang J (2008) Dopaminergic signaling in dendritic spines. Biochem Pharmacol 75:2055–2069

Zahm D (2000) An integrative neuroanatomical perspective on some subcortical substrates of adaptive responding with emphasis on the nucleus accumbens. Neurosci Biobehav Rev 24:85–105